Power-based localization in correlated log-normal fading aided by conditioning measurements

George Arvanitakis, Florian Kaltenberger
Eurecom
Sophia Antipolis, France
{George.Arvanitakis, Florian.Kaltenberger}@eurecom.fr

Ioannis Dagres[1], Andreas Polydoros[1&2]
1 Institute of Accelerating Systems and Applications, NKUA, Athens, Greece.
2 King Abdulaziz University, Jeddah, Saudi Arabia
{jdagres, polydoros}@phys.uoa.gr

Adrian Kliks
Poznan University of Technology
Poznan, Poland
akliks@et.put.poznan.pl

***Abstract*—The paper addresses the performance evaluation via the Cramer-Rao Lower Bound (CRLB) of power-based localization of a source in spatially-correlated log-normal propagation. The novel element is the inclusion and assessment of the impact of *conditioning measurements* on such performance. The proposed model parameterizes performance by both the sensor topology (density, positioning) producing the current measurements as well as by conditioning measurements (essentially, prior or training data) which reduce the statistical uncertainty in the model. Experimental results for indoor and outdoor environments are presented which quantify the expected localization accuracy, as well as identify practical issues to be further addressed. One main concern is the quantification of scaling on required sensor-network size for achieving a pre-specified localization accuracy.**

***Index Terms*—Received signal strength; localization; log-normal; spatial correlation, Cramer-Rao Lower Bound;**

I. INTRODUCTION

Transmitter localization via distributed sensor networks is an enabling technology for a large set of applications. In particular, radio-source localization is viewed as an important element of upcoming cognitive radio networks [1]. Endowed with the capability to sense and process radio activity in the surrounding environment, cognitive radios can efficiently plan, decide upon and execute their respective actions [2], [3].

Sensing is based on simple received power. In radio jargon this is called Received Signal Strength (RSS) and it is popular due to its simplicity every radio measures power. The flip side of this simplicity is that RSS-based localization tends to be less accurate than competing, more complex schemes. This is because, for RSS-based localization, deterministic power-law is not a reliable reception model. More advanced probabilistic (log-normal) propagation models include a shadow-fading random variable (rv) to describe the variation around the mean provided by the aforementioned power law. This is still not adequate, unless the spatial-correlation aspect of propagation is included in the model. Proper modeling information can be presumed available in modern networks endowed with databases which extract the information from past measurements or training and offer it for future benefits. The present paper incorporates this spatial correlation aspect and assesses its impact, in conjunction with the beneficial effect of prior training measurements. We adopt the term *conditioning measurements* (CM) to represent any such modeling enrichment or uncertainty reduction brought about by the availability of training, pilot-based information, past known results, or any other factor that will yield a conditional propagation density with better performance. Implicit in this conditioning is the existence of a sensor network that provided those, a network viewed as distinct from the currently available one for the collection of the present measurements. For compactness, the terms prior and current will be used to describe these two classes although, in a general setting, epoch may not be the only qualifier of information provision. A probabilistic (Bayes) flavor of the respective terms yields a better understanding.

Many models exist for describing spatial correlation in shadow fading [4]. Experiments have also been executed for measuring it [5] [6], and various techniques have been proposed for taking advantage of it in a solution [7]. Performance analysis and improvement of RSS-based localization in such an environment has been performed in [8], [9]. In [10], [11], the CRLB for Correlated Log-Normal (CLN) propagation was derived for different parameters. The novelty of the present paper is that it takes *spatial correlation* as well as CM into account for deriving the respective CRLB and then using it to assess performance. One of the main benefits of such parametric performance quantification is the ability to address questions of network scaling. In particular, we can address questions such as: (1) what is the required density of RSS-based sensor networks (prior and current) for achieving a given localization accuracy? (2) How can current required density be reduced in view of the utilization of the prior network? (3) How are these two network densities (prior and current) related in general, for a given propagation environment? Because the answers herein are based on rather simple analytic models for the propagation environment and the spatial statistics, another important question is (4) how close are these answers to the true performance typically experienced in practice? This last question is hard to answer, in general, because any given trial represents a single realization of the underlying stochastic experiment. There have been qualitative arguments [8] on the value of exploiting spatial correlation but to provide hard, quantitative arguments there needs to be more extensive

measurement campaigns. The indoor measurements of the present paper using the OpenAirInterface (OAI) [12] platform further add to the collection of such available results.

The paper is organized as follows: Section II presents the CRLB propagation model. The statistics of RSS are derived with the inclusion of CM, since these are needed for the derivation of the CRLB. In Section III, this CRLB is derived and is subsequently invoked in the semi-analytic performance assessment of Section IV. For drawing specific performance conclusions two scenarios are chosen, one indoor and one outdoor. Based on those, we can assess the additional gains enabled by CM. In section V, finally, we present the experimental gains observed from the OAI collection in an indoor environment.

II. PROPAGATION MODEL

RSS measurements are drawn either from a set of sensors in a prior network (which lead to CM) or from a current network. The current scenario assumes known sensor positions plus a single active emitter within an area of interest. This leads to three unknown parameters under estimation: two flat-plane coordinates plus the transmit power of the emitter.

We adopt the classic log-normal propagation model

$$R_i = P^{tx} - L_0 - 10\alpha log(d_i/d_0) + n_i^s + n_i^f \ , \qquad (1)$$

where R_i is the source power, measured by i-th sensor or RSS, $d_i = \|\mathbf{x}_i - \mathbf{s}\|$ is their respective distance ($\mathbf{x}_i$,$\mathbf{s}$ are the coordinates of i-th sensor and source, respectively), P^{tx} is the emitter power, d_0 is a reference distance and L_0 is the power loss in that reference distance, α is the path-loss exponent, n_i^f is the noise due to fast fading, which is hereby modeled as zero-mean Gaussian (in linear scale) and (n_i^s) is the shadow-fading rv. We follow common practice and reduce the effect of fast fading by averaging measurements taken around the true location. This maybe seem unpractical (since we don't know where the source is), but the same effect can be had by moving the sensors around a bit instead of the source. It follows the above log-normal distribution: a Gaussian rv in the log domain with zero mean and variance σ_s^2.

1) Typical power model in lognormal fading: The typical model used does not account for CM, plus the sensors are considered far apart from each another, with zero spatial correlation. Let $m_i(\theta) = P^{tx} - L_0 - 10\alpha log(d_i/d_0)$, then, for $\theta = [P^{tx}, L_0, d_0, \alpha, x, y]$ as the unknown parameters under estimation, we have

$$R_i = m_i(\theta) + n_i^s \ , \qquad (2)$$

so, R_i follows Gaussian pdf

$$P_i(R_i|\theta) = \frac{1}{(\sigma_s\sqrt{2\pi})} e^{\frac{-\left(R_i - m_i(\theta)\right)^2}{2\sigma_s^2}} \ . \qquad (3)$$

Due to zero spatial correlation, the joint pdf becomes

$$P(\mathbf{R}|\theta) = \prod_{i=1}^{N} P_i(R_i|\theta) \ , \qquad (4)$$

for the vector measurement $\mathbf{R} = [R_1, \cdots, R_N]$.

2) Power model in lognormal fading under CM: The propagation model is the same as above. In addition, let $R_i^{\{t\}}$ be the current measurement rv of the i-th sensor from the source at a location $\mathbf{t} = (x, y)$ and let $\mathbf{R}_i^{\{p\}}$ be the vector of M CM (say, derived from a training source and a prior sensor network) at locations $\mathbf{p} = [\mathbf{p}_1, \ldots, \mathbf{p}_M]$. The pdf for all measurements (in dB) is modeled as joint Gaussian:

$$\begin{bmatrix} R_i^{\{t\}} \\ \mathbf{R}_i^{\{p\}} \end{bmatrix} \sim N\left(\begin{bmatrix} \mu_i^{\{t\}} \\ \mu_i^{\{p\}} \end{bmatrix}, \begin{bmatrix} \sigma_i^{\{t\}} & \mathbf{C}_i^{\{t\times p\}} \\ \mathbf{C}_i^{\{p\times t\}} & \mathbf{C}_i^{\{p\}} \end{bmatrix} \right) \ , \qquad (5)$$

where

$$\begin{array}{c} \mu_i^{\{t\}} = P_T - 10\alpha log(d_i^{\{t\}}) \\ \mu_i^{\{p\}} = P_T - 10\alpha log(\mathbf{d}_p^{\{t\}}) \\ \sigma_i^{\{t\}} = \sigma^2 \end{array} \ , \qquad (6)$$

$$C_i^{\{p\}} = \sigma^2 \begin{bmatrix} \rho_i^{\{p_1\}} & \cdots & \rho_i^{\{p_1\times p_M\}} \\ \vdots & \ddots & \vdots \\ \rho_i^{\{p_M\times p_1\}} & \cdots & \rho_i^{\{p_M\}} \end{bmatrix} \ , \qquad (7)$$

and

$$C_i^{\{p\times t\}} = C_i^{\{t\times p\}^T} = \sigma^2 \begin{bmatrix} \rho_i^{\{p_1\times t\}} \\ \vdots \\ \rho_i^{\{p_M\times t\}} \end{bmatrix} \ . \qquad (8)$$

Here, $P_T = P^{tx} - L_0 - 10\alpha log(d_0)$ is a simplifying parameter, which assumes that the source(s) providing the CM and the current source have the same transmit power. $d_i^{\{t\}}$ is the unknown distance between the emitter and the i-th sensor and $\mathbf{d}_i^{\{p\}}$ is $M \times 1$ vector with the known distances between the i-th sensor and the positions of the CM (totally we have M CM positions). Also, $\rho_i^{\{p_k\times p_j\}} = e^{-\alpha_c d^{\{p\}}}$ is the correlation factor and $d^{\{p\}}$ is the distance between p_k and p_j pilot transmitters. The correlation constant is depicted as α_c and the de-correlation distance is defined as $d_c = 1/\alpha_c$. It is also assumed that the standard deviation of the shadow fading is equal for all sensors, i.e. $\sigma_i^{\{p\}} = \sigma$. Finally $\rho_i^{\{p_k\times t\}}$ is the correlation factor between the p_k pilot and the unknown transmitter.

Thus, the conditional pdf of $R_i^{\{t\}}$ given $\mathbf{R}_i^{\{p\}} = \mathbf{r}_i^{\{p\}}$ ($\mathbf{r}_i^{\{p\}}$ are the specific values of the CM) is also Gaussian $N\left(\mu_i^{\{t|p\}}, \sigma_i^{\{t|p\}^2}\right)$ with mean and variance given by

$$\begin{aligned} \mu_i^{\{t|p\}} &= E\left\{R_i^{\{t\}} | \mathbf{R}_i^{\{p\}} = \mathbf{r}_i^{\{p\}}\right\} \\ &= \mu_i^{\{t\}} - \mathbf{C}_i^{\{p\times t\}^T} \mathbf{C}_i^{\{p\}^{-1}} \left(\mu_i^{\{p\}} - \mathbf{r}_i^{\{p\}}\right) \ , \end{aligned} \qquad (9)$$

and

$$\sigma_i^{\{t|p\}^2} = \sigma^2 - \mathbf{C}_i^{\{p\times t\}^T} \mathbf{C}_i^{\{p\}^{-1}} \mathbf{C}_i^{\{p\times t\}} \ . \tag{10}$$

Therefore $\mathbf{R}^{\{t\}} \sim N\left(\mu\left(\theta\right), \mathbf{C}_s\left(\theta\right)\right)$, where

$$\mu\left(\theta\right) = \left[\mu_1^{\{t|p\}}, \mu_2^{\{t|p\}}, \cdots, \mu_N^{\{t|p\}}\right] \ , \tag{11}$$

is the $N \times 1$ mean vector and

$$\mathbf{C}_s\left(\theta\right) = \left[\begin{array}{ccc} \sigma_1^{\{t|p\}^2} & \cdots & 0 \\ \vdots & \ddots & \vdots \\ 0 & \cdots & \sigma_N^{\{t|p\}^2} \end{array}\right] \ , \tag{12}$$

is the $N \times N$ covariance matrix between the sensors, already calculated. Both depend on θ. In sum, the pdf of the received power is

$$\begin{aligned} P\left(\mathbf{R}^{\{t\}};\theta\right) = & \frac{1}{\left(2\pi\right)^{\frac{N}{2}} det\left[\mathbf{C}_s\left(\theta\right)\right]^{\frac{1}{2}}} \\ & \exp\left[-\frac{1}{2}\left(\mathbf{R}^{\{t\}} - \mu\left(\theta\right)\right)^T \mathbf{C}_s^{-1}\left(\theta\right)\left(\mathbf{R}^{\{t\}} - \mu\right)\right] \ . \end{aligned} \tag{13}$$

III. CRAMER-RAO LOWER BOUND

The Fisher information matrix for Gaussian rv is (see [13]):

$$\begin{aligned} \left[I\left(\theta\right)\right]_{kl} = & \frac{1}{2} tr\left(\mathbf{C}_s^{-1}\left(\theta\right) \frac{\partial \mathbf{C}_s\left(\theta\right)}{\partial \theta_k} \mathbf{C}_s^{-1}\left(\theta\right) \frac{\partial \mathbf{C}_s\left(\theta\right)}{\partial \theta_l}\right) \\ & + \frac{\partial \mu\left(\theta\right)^T}{\partial \theta_k} \mathbf{C}_s^{-1}\left(\theta\right) \frac{\partial \mu\left(\theta\right)}{\partial \theta_l} \ , \end{aligned} \tag{14}$$

which $tr()$ is the trace of the matrix. We thus need to calculate the partial derivatives

$$\frac{\partial \mathbf{C}_s\left(\theta\right)}{\partial \theta_k} = \left[\begin{array}{ccc} \frac{\sigma_1^{\{t|p\}^2}}{\partial \theta_k} & \cdots & 0 \\ \vdots & \ddots & \vdots \\ 0 & \cdots & \frac{\sigma_N^{\{t|p\}^2}}{\partial \theta_k} \end{array}\right] \ , \tag{15}$$

where

$$\begin{aligned} \frac{\sigma_i^{\{t|p\}^2}}{\partial \theta_k} = & -2\sigma_i^{\{t|p\}} \left[\frac{\partial C_i^{\{p\times t\}^T}}{\partial \theta_k} C_i^{\{p\}^{-1}} C_i^{\{p\times t\}}\right. \\ & \left. + C_i^{\{p\times t\}^T} C_i^{\{p\}^{-1}} \frac{\partial C_i^{\{p\times t\}}}{\partial \theta_k}\right] , \end{aligned} \tag{16}$$

and

$$\frac{\partial C_i^{\{p\times t\}}}{\partial \theta_k} = -\alpha_c e^{-\alpha_c d^{\{p_j\times t\}}} \frac{\partial d^{\{p_j\times t\}}}{\partial \theta_k} \ . \tag{17}$$

For $\theta_k = x^{\{t\}}$, (same for $y^{\{t\}}$)

$$\frac{\partial C_i^{\{p\times t\}}}{\partial x^{\{t\}}} = \frac{\alpha_c\left(x^{\{p\}} - x^{\{t\}}\right)}{d^{\{p_j\times t\}}} \rho_i^{\{p_j\times t\}} \ . \tag{18}$$

For the derivatives of the mean value we have

$$\begin{aligned} \frac{\partial \mu\left(\theta\right)}{\partial \theta_k} = & -10\alpha \frac{\partial \log_{10}\left(d_i^{\{t\}}\right)}{\partial \theta_k} - \frac{\partial C_i^{\{p\times t\}^T}}{\partial \theta_k} C_i^{\{p\}^{-1}} \\ & \left(P_T \mathbf{1}_M - 10\alpha \log_{10}\left(d_i^{\{p\}} - \mathbf{r}_i^{\{p\}}\right)\right) \ . \end{aligned} \tag{19}$$

We are now able to compute the CRLB (inverse of the Fisher information matrix) for given prior and current networks. To assess performance of a stochastic current network under a stochastic prior network, a semi-analytic approach is adopted.

IV. PERFORMANCE ASSESSMENT

The adopted approach averages over the random positions of both stochastic networks. This will be followed both without a prior network (sub-section A) as well as with (sub-section B).

A. Performance without CM

For the current network, under no preference for the source position, we place the latter in the middle of a square and model the random positions of the sensors. One such possibility is a two-dimensional Gaussian r.v. The means of all sensor positions will form a square grid of points based on the target density, and variance relative to that density. In all simulations we will assume that the transmitter lies at the center of this deployment, and the sensors capable of measuring its power are determined by a coverage area, a circle around the emitter. The radius of this coverage area is determined by the receive power sensitivity of the measurement network, the transmit power of the emitter, and the propagation characteristics (path-loss exponent).

The simulation process always begins with a very dense realization and gradually we expand the distances of the sensors until the point where less than three sensors are within the coverage area (we have three degrees of freedom (x, y, P), so we need at least three equations). The performance is measured for each step, averaged over different realizations.

Two different propagation scenarios will be examined, one called 'Indoor' and the other 'Outdoor', using respectively a parameterization that tries to reflect such scenarios, i.e. small coverage, de-correlation distance, large path-loss exponent for the indoor scenario and the opposite for the outdoor. The exact values used for those two scenarios are depicted in Table I.

TABLE I
PARAMETERIZATION OF THE PROPAGATION SCENARIOS

Parameters	**Scenarios**	
	Indor	Outdoor
Path loss	2	3
Shadow Fading	8	8
correlation coefficient (d_c)	2 $(0.5m)$	0.1 $(10m)$
Range (coverage)	$30dB$ $(3000m^2)$	$80dB$ $(0.6km^2)$

The semi-analytic performance assessment for these two scenarios is conducted by the following way. For a given density of deployment network random realizations of such networks are first produced, and then, based on the coverage,

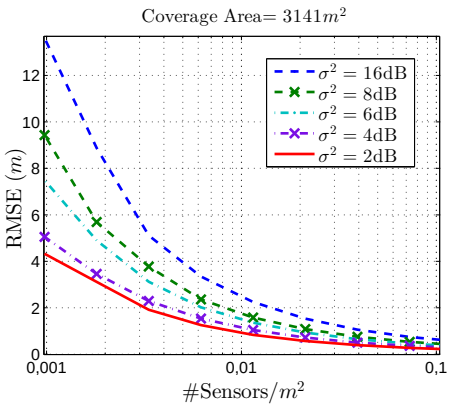

Fig. 1. Indoor scenario for different shadow fading values

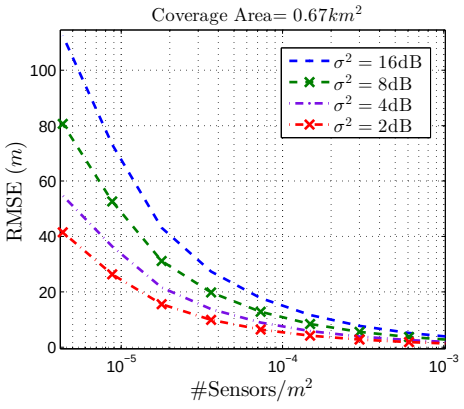

Fig. 2. Outdoor scenario for different shadow fading values

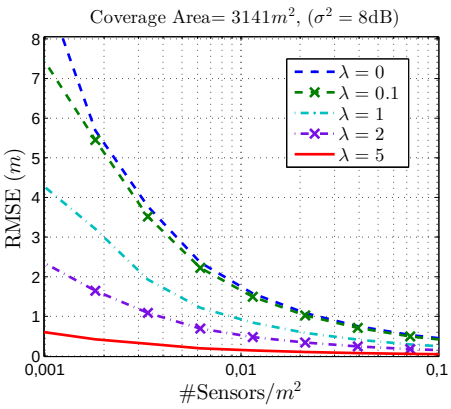

Fig. 3. Indoor scenario for various pilot placement cases and shadow fading equal to 8dB

the active sensors are selected. Based only on the active sensors, the CRLB is computed, and averaged over a large number of network realizations. The results for the indoor scenario and for different levels of shadow fading variance (2 to 16) are depicted in Fig. 1. The root mean square error (RMSE) is kept below 1 meter in most cases for a density of 1 sensor per 10 square meters, which is considered very dense. For the case of 1 sensor per $100m^2$, which is a rather sparse for indoor network, the error is bellow $4m$, a value that has been measured experimentally by our group in several measurement campaigns [14]. The coverage area of this example is $33m$, so a $4m$ RMSE is consider unacceptable.

For very sparse networks the shadow fading plays very important role, and only for very small values localization can be feasible.

For the outdoor scenario, the respective assessment is depicted in Fig. 2. The coverage radius in this scenario is 464 meters. The RMSE is small (bellow $6m$) for a rather high density network of 1 sensor per $1000m^2$ and bellow $20m$ for 1 per $10000m^2$. It is clear from the performance results depicted so far that the RSS-based localization for CR applications requires very high density sensor networks, if no CM are utilized.

B. Performance using CM

This is the most important part of our contribution, since we will examine how the CM can reduce the error and/or the density of the needed measurement network. The process is the same as in the previous section, but here we also have to average out the random positions of the CM. There exist many spatial models used for the positions of radios leading to different performances. Here we model the position of the CM as a homogenous Poisson Point Process (PPP) of a given density λ. The underline pilot density λ is the expected number of points (CM) of the process per unit area (one square meter for indoor and one thousand for outdoor scenario). The case without CM is also depicted ($\lambda = 0$). Starting from the 'indoor' scenario, the performance curves for various densities are provided. Fig. 3 depicts the case of indoor scenario (correlation distance of $0.5m$). Theory suggests huge improvement when having dense measurements. For the case of $\lambda = 5$, i.e. the density of the PPP process is 5 sensors per square meter the error is negligible even for very sparse sensor networks. The performance gain is negligible when the density falls below 1 measurement per $10m^2$. As we can see, the expected theoretical gain is huge; enough to enable practical use of RSS-based localization, as long as a dense measurement database of CM is available.

The performance for the 'outdoor' scenario is also depicted in Fig. 4.

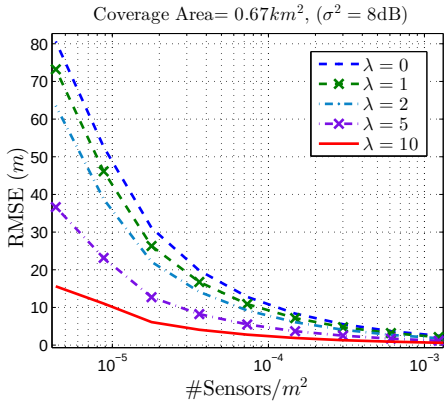

Fig. 4. Outdoor scenario for various pilot placement cases and shadow fading equal to 8dB

Equivalent performance enhancement is displayed. When the density is higher than 1 per $100m^2$ the RMSE is bellow $10m^2$ even for very sparse sensor networks. The performance gain is negligible when the density falls below 1 per $1000m^2$.

What we can see is that in theory, the potential of performance enhancement is large when having access to CM with density at the order of the de-correlation distance. What the theory does not say, is the method of getting such performance. The CRLB characterizes the performance of the ML estimator, which is a non-convex optimization problem.

V. EXPERIMENTAL RESULTS

Using semi-analysis we were able to examine how the performance scales without the need to set-up large costly experimental campaigns. How close this view to the reality depends on the modeling assumptions. The simplicity of the adopted model does not allow us to make any strong conclusion. Experimental campaigns are needed to verify, at least, the tendencies. An experimental campaign at an indoor environment is presented herein in order to practically assess the gains of the spatial correlation. Due to space limitation, we cannot provide a detail mathematical description of each processing step.

The set-up was the following: for the sensor network we used one OAI platform, controlling four antennas, each one acting as a different sensor (Rx) located far apart from each other (with lengthy cables). A signal generator was used as a transmitter (Tx) to be localized. The signal generator was tuned at the same central frequency (F_c) with the sensors. Characteristics of Tx and Rx are shown at Table II.

TABLE II
TRANSMITTER / RECEIVER CHARACTERISTICS

Transmitting signal	Receiver antennas
Random OFDM symbols	Fc = 1.9076 GHz
0dBm power	Gain = 20dB
Isotropic at (x-y) plate	Isotropic at (x-y) plate
Bandwidth = 5 MHz	

Tx was placed at totally 1846 different positions (grid with step 10cm), blue dots, as we see at Fig. 5. Red dots depicts the positions of four Rxs. The total area for this experiment was $\approx 130m^2$. The high density of the measurement campaign covers two purposes. The first one is the need to average out the fast fading. The second one is the need to measure the shadow fading correlation. For the fast-fading averaging, we used 9 neighbor points to produce one. This reduced the grid density, from a $10cm$ step to $30cm$. This $30cm$ is the granularity of our measurement campaign for estimating the spatial correlation.

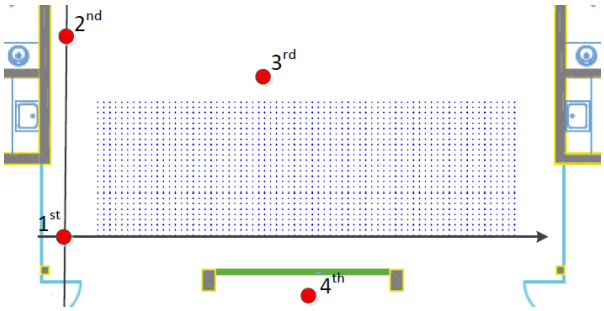

Fig. 5. Set up of the experimental procedure, red dots indicate the Rxs positions and blue dots the different Tx positions

A different processing procedure was followed in order to visualize this correlation by using a two dimensional moving average filter directly on the dense measurements. The results are depicted in Fig. 6 for Rxs 1 & 3, where the parameters of the propagation model were estimated by a simple least-squares fit. The correlation can be seen visually. Taking also into account the positions of the Rxs, the existence of angular correlation is also evident.

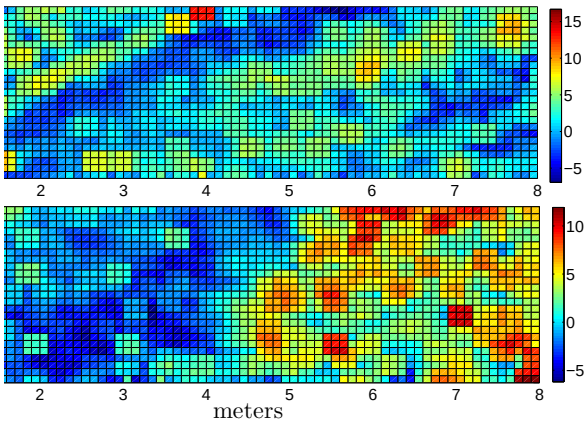

Fig. 6. Shadow Fading for Rx1 (up) and Rx3 (down)

Another question that arises regarding the modeling relates to the Gaussianity of the shadow fading. Fig. 7 shows the histogram of shadow fading variables for the second Rx and the Gaussian fitting curve. The amount of points is not enough for a smooth result, but the tendency on following a Gaussian distribution can be verified. The model parameters (path-loss, shadow-fading variance) for each Rx is different as opposed to the theoretical modeling assumptions where it was consider the same.

As next step we calculate the de-correlation distance of the environment. At Fig. 8 we depict the estimated correlation with respect to distance for all Rxs. The average de-correlation distance is $d_c \approx 0.65m$.The minimum de-correlation value is $\approx 0.3m$, observed, as expected, for the non-line of sight Rx (#4). We should mention that without the fast-fading averaging, the de-correlation distance is less than $7cm$.

Lastly: what is the performance gain when exploiting CM. We follow an assessment based on the CRLB. More specifically a slight modification of it to support the different propagation parameters per sensor (another deviation from the theoretical model). The key parameter in this assessment is the estimated shadow fading variance (per sensor). Without the CM the shadow fading is modeled as zero-mean. This is not the case with CM.

Using various interpolation techniques (for a given set of CM) we estimate the mean, and then the shadow fading variance that best describes the measurements. The interpolation techniques used for this scope are three deterministic (Linear, Voronoi regions, and Weighted Voronoi [15]) and one probabilistic (Kriging [15]).

In theory, we choose PPP to model the random position of the CM. Here, we can simulate the probabilistic nature of the CM positions by taking randomly a given portion of the measurements and use them as CM. The process for

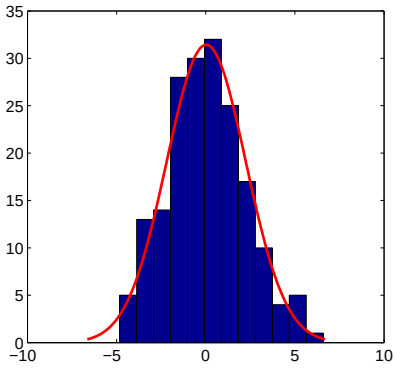

Fig. 7. Histogram of Shadow Fading

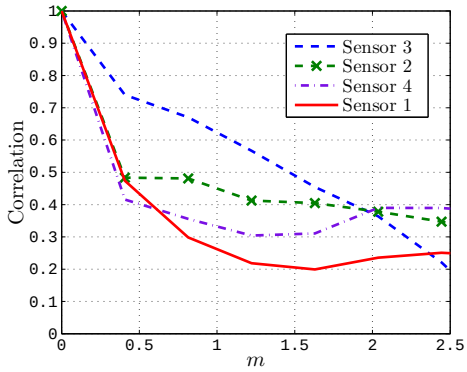

Fig. 8. Correlation wrt distance

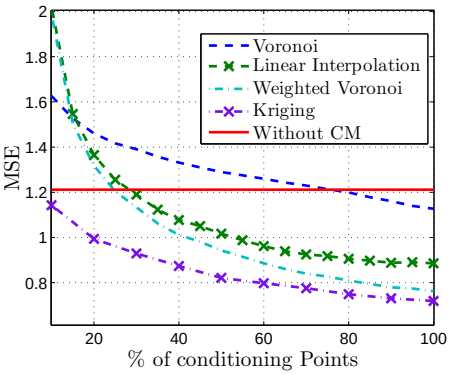

Fig. 9. Variance for each Interpolation Method

computing the CRLB of each point depicted in Fig. 9 is the following: For the given percentage X (x-axis) and for each point P, we randomly choose $X\%$ of the measurements (also excluding the measurement on point P). Using these measurements as CM the new mean of the shadow-fading of point P is estimated (by spatial interpolation), and by this the new shadow-fading error term. This process is repeated many times and for each point P. By this process we are able to estimate the new shadow fading variance, for each choice of interpolation method, and for the given CM density.

Fig. 9 depicts the CRLB (Mean Square Error, MSE) for a reference point at the center of the room, as a function of $X\%$. As expected, the probabilistic interpolation (Kriging) method gives the best performance, which is gradually converges to the case with no CM. The linear interpolation method provide better performance only for dense CM. The Voronoi methods on the other hands provide a good trade-off between performance and complexity.

As a final comment, we can say that in practice, for indoor environments, same performance gain is verified. Due to the small de-correlation distance, the density of our measurements did not allowed as to observe the huge gains promised by theory. This means that for indoor environments extremely dense CM is need it.

VI. CONCLUSIONS AND FUTURE WORK

In this work we have provided an assessment of the required network density of sensors for RSS-based localization utilizing CM in log normal environment with spatial correlation. Using the CRLB and proper semi-analysis we showed that large performance gains are expected when the spatial correlation is exploited by the use of a database of CM. The utilization of CM is been used very often in the literature, but a semi-analytic approach that reveals the scaling of the needed sensor network is for the first time introduced. The results of an experimental assessment using the OAI platform are also presented, focusing on the practical utilization of the spatial shadow-fading correlation. As future work, we have to expend the theoretical results and to rearrange a measuring campaign at the more challenging multi source scenario.

ACKNOWLEDGMENT

This work was supported by the NEWCOM# NoE of the EC Seventh Framework Programme (FP7-ICT-318306)

REFERENCES

[1] J. Mitola, "Cognitive radio - an integrated agent architecture for software defined radio," *Royal Institute of Technology (KTH)*, may 2000.

[2] P. Casadevall *et al.*, "Radio environmental maps: information models and reference model. document number d4.1," 2012.

[3] D. Denkovski, V. Rakovic, M. Pavloski, K. Chomu, V. Atanasovski, and L. Gavrilovska, "Integration of heterogeneous spectrum sensing devices towards accurate rem construction," in *Wireless Communications and Networking Conference (WCNC), 2012 IEEE*, April 2012, pp. 798–802.

[4] M. Gudmundson, "Correlation model for shadow fading in mobile radio systems," *Electronics Letters*, vol. 27, no. 23, pp. 2145–2146, Nov 1991.

[5] N.-R. Jeon, K.-H. Kim, J.-H. Choi, and S.-C. Kim, "A spatial correlation model for shadow fading in indoor multipath propagation," in *Vehicular Technology Conference Fall (VTC 2010-Fall), 2010 IEEE 72nd*, Sept 2010, pp. 1–6.

[6] C. Oestges, N. Czink, B. Bandemer, P. Castiglione, F. Kaltenberger, and A. Paulraj, "Experimental characterization and modeling of outdoor-to-indoor and indoor-to-indoor distributed channels," *Vehicular Technology, IEEE Transactions on*, vol. 59, no. 5, pp. 2253–2265, Jun 2010.

[7] M. Bshara, U. Orguner, F. Gustafsson, and L. Van Biesen, "Fingerprinting localization in wireless networks based on received-signal-strength measurements: A case study on wimax networks," *Vehicular Technology, IEEE Transactions on*, vol. 59, no. 1, pp. 283–294, Jan 2010.

[8] D. B. Maja Stella, Mladen Russo, "Rf localization in indoor environment," vol. 21, no. 2, pp. 557–567, June 2012.

[9] R. Vaghefi and R. Buehrer, "Received signal strength-based sensor localization in spatially correlated shadowing," in *Acoustics, Speech and Signal Processing (ICASSP), 2013 IEEE International Conference on*, May 2013, pp. 4076–4080.

[10] L. Mailaender, "Geolocation bounds for received signal strength (rss) in correlated shadow fading," in *Vehicular Technology Conference (VTC Fall), 2011 IEEE*, Sept 2011, pp. 1–6.

[11] N. Patwari and P. Agrawal, "Effects of correlated shadowing: Connectivity, localization, and rf tomography," in *Information Processing in Sensor Networks, 2008. IPSN '08. International Conference on*, April 2008, pp. 82–93.

[12] *OpenAir Interface, http://www.openairinterface.org/.*

[13] S. Kay, *Fundamentals of Statistical Signal Processing, Volume I: Estimation Theory*, 1993.

[14] I. Dagres, A. Polydoros, D. Denkovski, M. Angjelicinoski, V. Atanasovski, and L. Gavrilovska, "Algorithms and bounds for energy-based multi-source localization in log-normal fading," in *Globecom Workshops (GC Wkshps), 2012 IEEE*, Dec 2012, pp. 410–415.

[15] R. Hemsley, "Interpolation on a magnetic field," Tech. Rep., Sept 2009.